

Global maximum power point tracking of PV arrays under partial shading conditions using a modified particle velocity-based PSO technique

ISSN 1752-1416

Received on 15th October 2016

Revised 28th September 2017

Accepted on 15th December 2017

E-First on 5th February 2018

doi: 10.1049/iet-rpg.2016.0838

www.ietdl.org

Tanuj Sen¹, Nataraj Pragallapati²✉, Vivek Agarwal², Rajneesh Kumar¹¹Electrical and Electronics Engineering Department, Birla Institute of Technology and Science-Pilani, Pilani, Rajasthan, India²Department of Electrical Engineering, Indian Institute of Technology-Bombay, Mumbai, Maharashtra, India

✉ E-mail: nataraj.wgdt@gmail.com

Abstract: Modern PV arrays are generally designed with bypass diodes to avoid damage. However, such arrays exhibit multiple peaks in their P - V characteristics under partial shading conditions. Owing to the limitation in the abilities of conventional maximum power point tracking algorithms in such cases, the application of other optimisation algorithms has been explored. This study proposes a modified particle velocity-based particle swarm optimisation (MPV-PSO) algorithm for tracking the global power peak of the multiple peak P - V characteristics. The MPV-PSO algorithm is both adaptive and deterministic in nature. It eliminates the inherent randomness in the conventional PSO algorithm by excluding the use of random numbers in the velocity equation. The proposed algorithm also eliminates the need for tuning the weight factor, the cognitive and social acceleration coefficients by introducing adaptive values for them which adjust themselves based on the particle position. These adaptive values also solve problems like oscillations about the global best position during steady-state operation and particles getting trapped in local minima. The effectiveness of the proposed MPV-PSO algorithm is validated through MATLAB/Simulink simulations and hardware experiments.

1 Introduction

A single PV module can produce as much current and voltage as its short circuit current and its open circuit voltage, respectively, which are generally low. PV modules are connected in a series-parallel (SP) configuration to produce the required amount of voltage and current. Under partial shading condition (PSC), shaded modules connected in series with unshaded modules may become reverse biased, causing them to overheat and get damaged. Thus, bypass diodes and blocking diodes are used to protect the modules and strings from excess currents. However, the usage of bypass diodes causes the P - V characteristics to exhibit multiple peaks under PSC, with one of them being the global peak (GP). The main motive of maximum power point tracking (MPPT) algorithms is to operate the system at the GP to draw the maximum amount of power from the system and ensure maximum efficiency [1].

Several MPPT techniques exist, the most notable among them being the hill climbing/perturb and observe (P&O) algorithm [2] and the incremental conductance (INC) [2, 3] algorithm. All these MPPT methods consider the characteristic slanted bell-shaped appearance of the P - V curve to determine the maximum power point (MPP). In [4], an adaptive P&O algorithm is presented which makes use of fuzzy logic control to change the operating point according to changes measured in power and voltage. The authors in [5, 6] present a comparative analysis of the P&O and INC algorithms for various frequencies of operation and voltage steps and conclude that the algorithms are similar in nature and functioning. These methods are not able to distinguish between peaks. This is a major problem under PSC as the P - V characteristics exhibit multiple peaks. If the initial point is not located close to the GP, the algorithm will track one of the local peaks leading to reduced operational efficiency.

Aside from these conventional MPPT techniques, other methods have also been applied to track the GP under PSCs [7, 8]. In [9], the authors present an artificial neural network (ANN) technique to recognise the location of the GP. The problem with the usage of ANN for global MPPT (GMPPT) is that the network weights must be properly tuned using a large amount of training data. The authors present a new method for GMPPT in [10], where

the DC-DC converter is controlled to behave as a constant input power load. Other techniques such as DIRECT search [11] and the two-step method [12] for GMPPT have also been presented. Another technique known as the restricted voltage window search for GMPPT has been presented in [13] and it involves reducing the size of the search space to facilitate faster tracking of the GP.

Evolutionary algorithms derived from the behaviour of swarms/colonies are finding increased applications in the field of GMPPT under PSC. The most popular among these algorithms which has found extensive use for GMPPT under PSC is the particle swarm optimisation (PSO) algorithm due to its simplistic nature. Many modifications have been proposed to the conventional PSO (C-PSO) to make it much more suited to GMPPT purposes [14–17]. In [14], the authors have proposed a PSO-based GMPPT with reduced steady-state oscillations using direct duty-cycle control. The authors in [15] have also proposed a method to employ the C-PSO to find the GMPP. Also, to reduce the time for tracking the GMPP, they have suggested a method to reduce the search space for the PSO algorithm by tracking the first local peak using P&O technique. Other methods involving PSO have also been proposed [16, 17]. The velocity equation of PSO depends on random numbers and that the weight factor, social and cognitive coefficient need to be chosen with proper consideration, otherwise large step sizes may arise initially and the algorithm may take longer to reach steady state [17].

This paper proposes a modified particle velocity-based PSO (MPV-PSO) algorithm for tracking the GMPP and to overcome the drawbacks of the existing PSO techniques. The proposed MPV-PSO algorithm is deterministic in the sense that the random numbers in the velocity equation have been eliminated and there is no need to tune any of the parameters in the equation. The parameter values vary adaptively based on the position of the particles in the search space and their distance from the global best position. This proposed algorithm can perform well for static and dynamic tracking of GMPP and has the advantages of reduced steady-state oscillations about the GP, avoiding particle trapping in local minima.

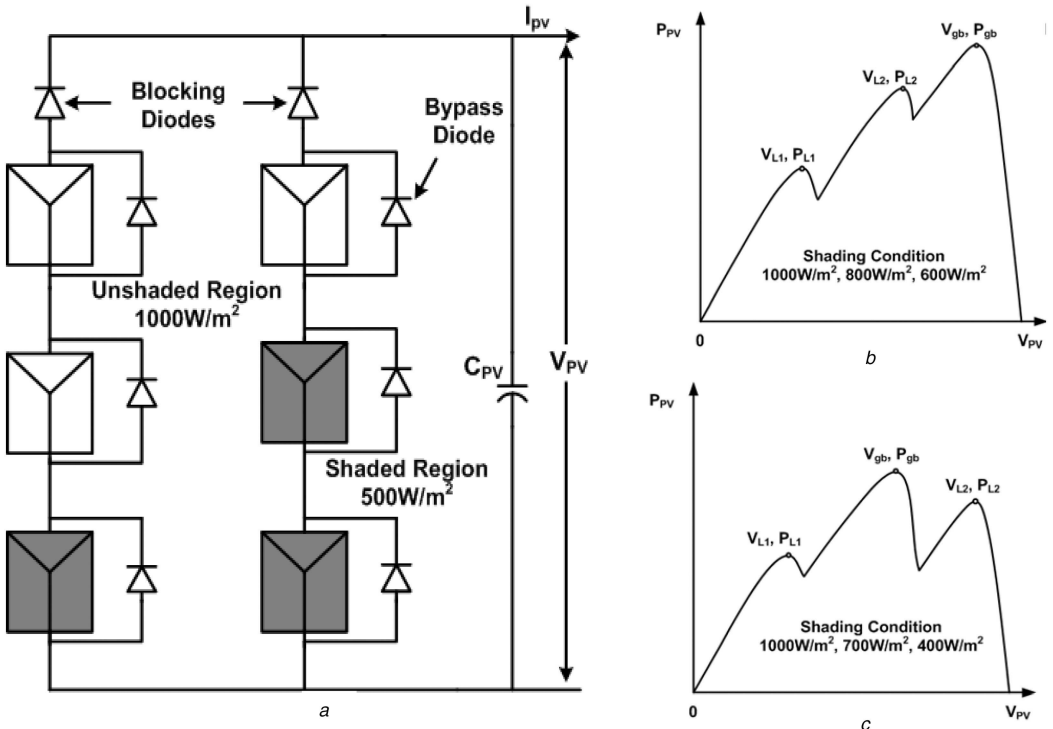


Fig. 1 Characteristics of PV array

(a) PV array of six PV modules in SP configuration, (b) P–V characteristics of PV array for right peak PSC, (c) P–V characteristics of PV array for middle peak PSC

2 Characterisation of PV array under PSCs

In case of non-uniform irradiation (due to PSC), for the series connected configuration employing bypass diodes [Fig. 1a], the P–V characteristics exhibit multiple peaks, with one of the peaks being the GP. This phenomenon of multiple peaks appearing in the P–V characteristics can be explained by considering a three PV module series string having different irradiation levels (PSC-I: 1, 0.8, 0.6 kW/m²) and (PSC-II: 1, 0.7, 0.4 kW/m²) as shown in Figs. 1b and c. (V_{L1} , P_{L1}) and (V_{L2} , P_{L2}) are the PV voltage and PV power values corresponding to the two local power peaks. (V_{gb} , P_{gb}) is the available PV voltage and PV power at the global power peak.

For the shading condition (PSC-I), there are three peaks ((V_{L1} , P_{L1}), (V_{L2} , P_{L2}), (V_{gb} , P_{gb})) in the P–V characteristics as shown in Fig. 1b. It consists of one GP (P_{gb}) and two local power peaks (P_{L1} and P_{L2}) and the corresponding voltages are $V_{gb} > V_{L2} > V_{L1}$ (i.e. the GP is the peak with the highest operating voltage). The P–V characteristics for the PSC-II, shown in Fig. 1c, consist of one global and two local power peaks with corresponding voltages $V_{L1} < V_{gb} < V_{L2}$ (i.e. the middle peak represents the GP). Thus, the P–V characteristics pattern of any PV array depends on the PSC. Therefore, the objective of finding the GMPP is a multi-modal optimisation problem. Thus, efficient optimisation algorithms are necessary for tracking the GMPP. In this paper, the PSO technique is used for determining the optimum solution.

3 Modified particle velocity-based PSO GMPPT algorithm

3.1 Conventional PSO

The PSO algorithm searches the entire solution space for candidate solutions and determines the best out of those solutions by a series of comparisons of the fitness values of these solutions. The behaviour of the member particles in PSO emulates that of the members of a swarm, wherein the particles try to move towards the best solution, while memorising the best solution encountered by them during their movement towards the best solution [18].

The particles are initially assigned some position in the solution space. The particle position is updated using the following equation [18]:

$$x_i^{k+1} = x_i^k + \text{vel}_i^{k+1} \quad (1)$$

where x_i^k defines the position of the particle in the current cycle and x_i^{k+1} is the updated particle position to be considered for the next cycle. vel_i^{k+1} is the update velocity of the particle for the current search cycle. The update velocity's magnitude and direction depend on certain factors and are determined by the following relation:

$$\text{vel}_i^{k+1} = w \cdot \text{vel}_i^k + c_1 r_1 (x_{lb_i} - x_i^k) + c_2 r_2 (x_{gb} - x_i^k) \quad (2)$$

The factor $c_1 r_1 (x_{lb_i} - x_i^k)$ is called the cognitive factor and considers the distance of the particle from its local best position, x_{lb_i} . The x_{lb_i} of a particle is the best position encountered by it while moving towards the best solution. The social factor enables the particles to move towards the global best solution. The global best position (GBP), (x_{gb}), is the best position encountered among all the particles from the start to the current cycle. There is also a weight or inertia factor, w which affects the update velocity in such a way so that the particle keeps moving in the same direction as in the previous cycle. c_1 and c_2 are the cognitive and social acceleration coefficients. Their values can be selected in the range (0, 2]. r_1 and r_2 are random numbers ranging between 0 and 1.

3.2 Modified PSO algorithm

The C-PSO algorithm has some parameters whose values must be selected by the programmer within a given range. The PSO also makes use of random numbers in the velocity equation which makes the results of the PSO unpredictable. This provides ample scope to introduce modifications into the existing PSO algorithm to make it more deterministic in nature with better and predictable results. Introducing suitable modifications may also make the PSO algorithm much more efficient in tracking the GMPP under PSC. This paper proposes such modification to the PSO equation which improves its performance, especially for the case of GMPPT under PSC.

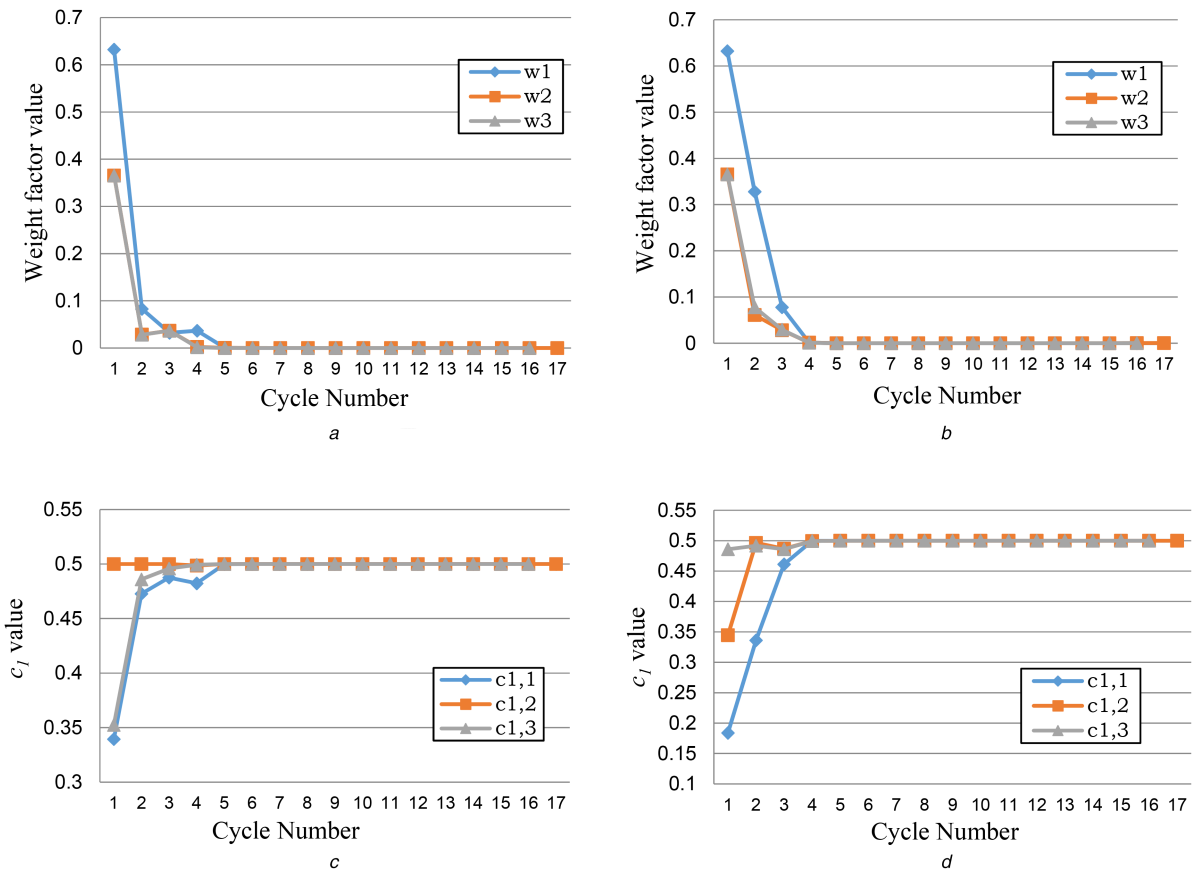


Fig. 2 Simulation results of the proposed MPV-PSO-based GMPPT under PSC

(a) Weight factor (w_i) value used in the update velocities of three particles for PSC of 1, 0.7, 0.4 kW/m², (b) Weight factor (w_i) value used in the update velocities of three particles for PSC of 1, 0.8, 0.6 kW/m², (c) Cognitive acceleration coefficient ($c_{1,i}$) values used in the update velocities of three particles for PSC of 1, 0.7, 0.4 kW/m², (d) Cognitive acceleration coefficient ($c_{1,i}$) values used in the update velocities of three particles for PSC of 1, 0.8, 0.6 kW/m²

3.2.1 Adaptive weight factor: The value of the weight factor sets the contribution of the old update velocity in the new velocity value. The weight factor proves helpful to keep the particle moving when it encounters a local peak or when it gets trapped in some local minima. The problem with this weight factor is that its value remains constant. As a result, it leads to sustained oscillations even when all the particles have converged to the GP because the particle velocities have a non-zero value.

In order to preserve the advantages of the weight factor as well as to reduce its negative effects on the convergence of the algorithm, an adaptive weight factor is presented. This adaptive weight factor lets its value to be dependent on the spread of the particles across the search space. The adaptive weight factor is given as follows:

$$w^k = \frac{V_{\max} - V_{\min}}{V_{oc}} \quad (3)$$

In (3), w^k is the weight factor value for the k th cycle. V_{\max} refers to the present location of the rightmost particle in the search space while V_{\min} is the present location of the leftmost particle. V_{oc} is the rated open circuit voltage of the PV array. An advantage of using this adaptive weight factor is that the programmer does not have to set its value every time the algorithm is reinitialised, making the modified algorithm much more self-sufficient. The variation of this adaptive weight factor with respect to the cycle number is presented in Figs. 2a and b.

3.2.2 Adaptive cognitive acceleration coefficient: The cognitive acceleration coefficient c_1 together with the random number r_1 determines the contribution of the cognitive factor to the update velocity value. The value of c_1 is also left to be selected by the programmer.

Initially, when particles are far from the GBP, there may be multiple minima located in between. Thus, the value of c_1 must be kept low to avoid particles from trapping in the local minima. As the particle moves closer to the GBP, the number of minima lying in between decreases, so c_1 value can be gradually increased to reduce convergence time. The new adaptive value of c_1 is made dependent on the distance of the particle from the GBP so that it can emulate the desired behaviour as described above and is given by the following formula:

$$c_{1,i}^k = 0.5 \left(1 - \frac{|x_{gb} - x_i^k|}{V_{oc}} \right) \quad (4)$$

Each particle has its own independent value of c_1 . The constant 0.5 limits the maximum value attainable by c_1 to be 0.5. This ensures that the c_1 is always less than or equal to half of the c_2 so that the cognitive factor is never able to dominate over the social factor and pull the particle farther from the GBP, especially for cases when the particle lies in a local minimum. The use of such a formula for c_1 relieves the programmer from the task of properly tuning its value before every run. Figs. 2c and d illustrate the variation of the adaptive cognitive acceleration coefficient with the execution of the algorithm for different PSCs.

3.2.3 Adaptive social acceleration coefficient: The social factor's involvement in the update velocity depends on the social acceleration coefficient, c_2 . The fact that the value of c_2 has to be properly tuned before running the algorithm reduces its elegance and introduces the need for tedious testing. In order to make the algorithm free from tuning requirements, the following formula for the value of c_2 is proposed:

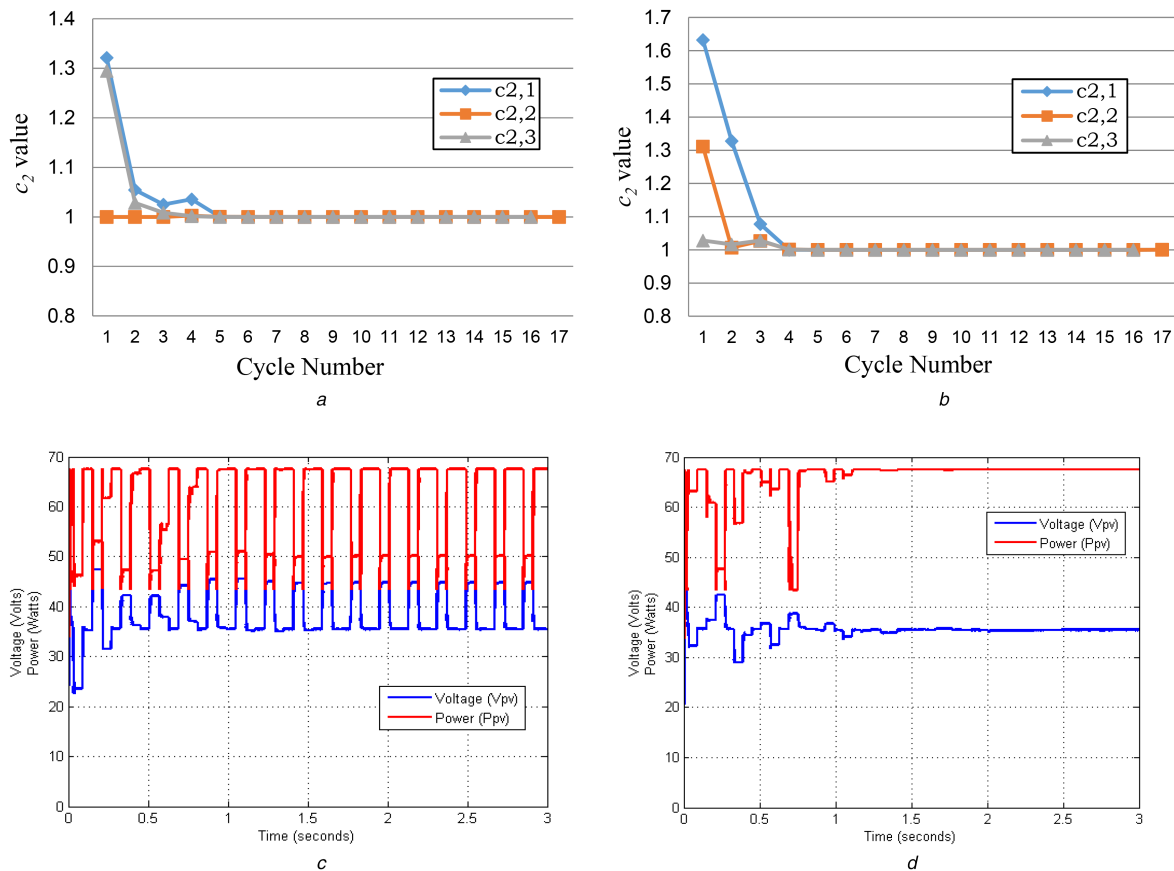


Fig. 3 Simulation results of the proposed MPV-PSO-based GMPPT under PSC social acceleration coefficient ($c_{2,i}$) values used in the update velocities of the three particles when using the proposed MPV-PSO for searching the GMPP under PSC

(a) Social acceleration coefficient ($c_{2,i}$) values used in the update velocities of three particles for PSC of 1, 0.7, 0.4 kW/m², (b) Social acceleration coefficient ($c_{2,i}$) values used in the update velocities of three particles for PSC of 1, 0.8, 0.6 kW/m², (c) Power and voltage traces versus time for GMPPT by using conventional PSO algorithm for the PSC: 1, 0.7, 0.4 kW/m², (d) Power and voltage traces versus time for GMPPT by using MPV-PSO algorithm without including the adaptive weight factor for the PSC: 1, 0.7, 0.4 kW/m²

$$c_{2,i}^k = \left(1 + \frac{|x_{gb} - x_i^k|}{V_{oc}} \right) \quad (5)$$

The formula presented above does away with the requirement for properly tuning c_2 every time the algorithm is run. Each particle has its own value of c_2 . The above formula allows c_2 to range between 1 and 2. It ensures that c_2 's magnitude is higher in the initial stages, when the particles are spread far apart, so that they can reach the GBP faster. When the particles are close to the GBP, c_2 's value tends to 1 to reduce the unwanted oscillations about the GBP. Figs. 3a and b illustrate the variation of the adaptive c_2 with the execution of the PSO algorithm for different PSC's. r_2 is eliminated from the update velocity equation to make the algorithm deterministic in nature.

Fig. 3c presents the simulation results which show that improper tuning of c_1 and c_2 can lead to local minima trapping when using the C-PSO as shown in Fig. 3a and how the adaptive values of c_1 and c_2 in MPV-PSO alleviate the problem of particles getting trapped in the local minima, presented in Fig. 3d.

Thus, the particle velocity equation for the MPV-PSO algorithm is given as follows:

$$\text{vel}_i^{k+1} = w^k \cdot \text{vel}_i^k + c_{1,i}^k(x_{lb_i} - x_i^k) + c_{2,i}^k(x_{gb} - x_i^k) \quad (6)$$

3.2.4 Velocity limiting: When the peaks in the $P-V$ characteristics are more and the initial distance between the particles is large, the update velocity may attain large values which may cause the particles to skip some intermediate peaks, out of which one may be the GP. This will lead to erroneous tracking of the GMPP. Therefore, to ensure that none of the peaks are skipped during the

searching process, the update velocity magnitude is limited to a maximum value presented below:

$$0 < |\text{vel}_i^k| < V_{\max} \quad (7)$$

$$V_{\max} = (0.8 \cdot V_{oc})/N \quad (8)$$

It has been shown in [8] that the peaks of the $P-V$ characteristics under PSC for a PV array are separated by a value approximately equal to V_{\max} . This value ensures that none of the peaks are skipped while exploring the search space for GMPPT. N is the number of PV modules connected in a PV string.

3.3 Implementation of MPV-PSO algorithm

The implementation of the MPV-PSO algorithm for GMPPT is presented in Fig. 4a in the form of a flowchart. The execution of the flowchart can be considered separately as three dependent modules which are linked to one another.

Three particles (V_1 , V_2 , V_3) signifying PV array reference voltages are initialised as the first step to implement this proposed MPV-PSO algorithm. The reference voltages are given in Fig. 4a. The selection of such values as the particle positions ensures that the entire search space is covered. The entire process continues so long as the GMPPT is reached. A condition has been provided to check if the GMPPT has been reached. If this condition is satisfied, the execution of the variable step P&O algorithm [19] is initiated to operate the PV array at the GMPP, where the voltage step is varying in proportion to the value of the derivative, dP_{pv}/dV_{pv} .

If there is a change in the PSC's and the accompanying power change (ΔP_{pv}) at the operating point is greater than a critical value (P_{crit_s}), the algorithm is reinitialised again. The algorithm is

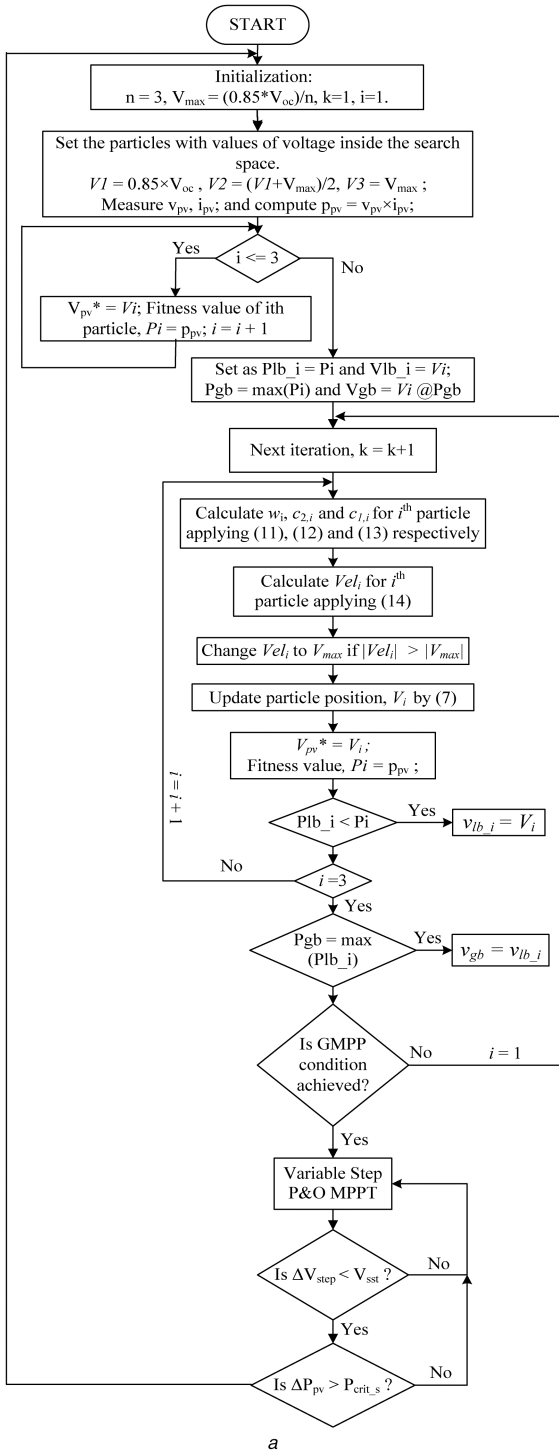


Fig. 4 Implementation of proposed PSO-based GMPPT control

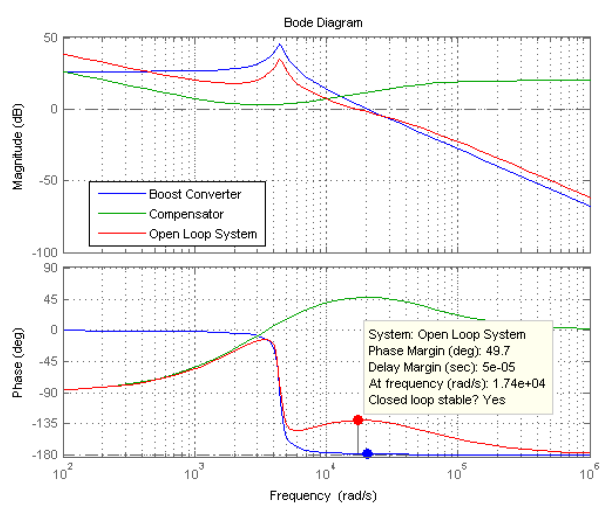
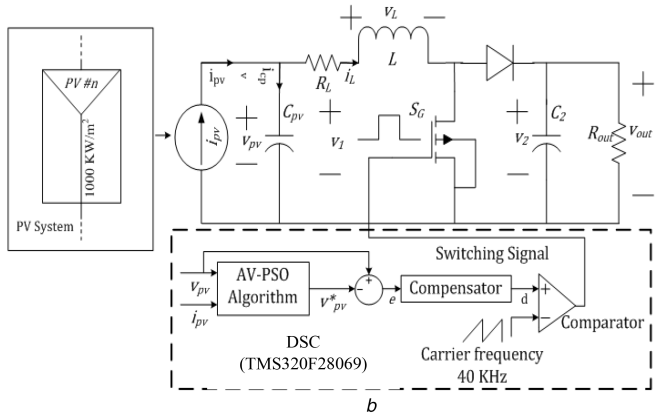
(a) Flowchart of the proposed MPV-PSO algorithm for GMPPT under PSC, (b) Control block diagram of MPP tracker circuit (boost converter) for generation of gate pulses, (c) Bode plots of boost converter: Compensator and open loop system

reinitialised only when it is ensured that the variable step P&O algorithm has also reached its steady state (voltage steps being very small). This is done to avoid the main algorithm from being reinitialised again and again when the irradiation conditions are in the process of changing. The control shifts to the beginning of the flowchart to reset the particle positions, the local best positions and the GBP and to subsequently run the MPV-PSO algorithm is again for tracking the new GMPP.

4 Simulation results and discussions

4.1 MPPT unit

The operating point of the PV array is controlled through a boost converter [20], as shown in Fig. 4b. This can be done by varying



the effective resistance across the output terminals of the PV array which in turn depends on the duty cycle. The compensator in Fig. 4b modulates the duty cycle of the DC-DC converter. For designing the compensator, the transfer function of the converter is to be determined. The plant transfer function of the converter, $T_p(s)$, is provided in Table 1 and was derived using small signal state space averaging. The negative sign of $T_p(s)$ should be taken into consideration when evaluating the error signal. The compensator, $G_c(s)$, is designed to ensure a stable closed loop response. The loop gain specifications and its transfer function are given in Table 1.

Table 1 Frequency domain specifications and transfer functions of the designed boost converter

Loop gain specifications	Phase margin (P.M.): 45°, phase crossover frequency (ω_c): 10% of the switching frequency (f_s)
$T_p(s) = \frac{\tilde{v}_{pv}(s)}{\tilde{d}(s)}$	$= \frac{-V_o \cdot (1/LC_{pv})}{s^2 + (1/R_{mpp}C_{pv}) \cdot s + (1/LC_{pv}) \cdot ((R_L/R_{mpp}) + 1)} = \frac{-122.523(3.333 \times 10^6)}{s^2 + 496.7s + 1.989 \times 10^7}$
$G_c(s)$	$(0.2) \cdot \left(\frac{s + 2.07 \times 10^3}{s} \right) \cdot 10 \cdot \left(\frac{s + 4.9821 \times 10^3}{s + 4.9821 \times 10^4} \right)$

Table 2 Different cases of PSC for simulation validations

Cases	Shading pattern	PV#1, kW/m ²	PV#2, kW/m ²	PV#3, kW/m ²
Case I	PSC-1	1	0.8	0.6
Case II	PSC-2	1	0.7	0.4
Case III	PSC-2 to PSC-1 at $t = 2$ s			

4.2 Simulation results of PV array under PSC

The simulations for testing the performance of MPV-PSO algorithm for GMPPT under PSC have been carried out in MATLAB-Simulink. The simulations have been carried out for three different cases of PSC for a three-module series connected PV string. The system details are given in Table 2.

Case I: For this case, the shading pattern was set as PSC-1, causing the rightmost of the three peaks of the P - V characteristics to be the GP. Fig. 5a shows the results using the C-PSO algorithm for GMPPT, whereas Fig. 5b shows the results for the proposed MPV-PSO algorithm. It is evident from these results that the C-PSO takes a considerably longer time to track the GP. While the C-PSO takes almost ten cycles, i.e. 10×3 (because we are using three particles) = 30 times of MPPT sample time (T_{mpp}), the MPV-PSO algorithm takes only three cycles ($=3 \times T_{mpp}$) to track the GP. Here, the GMPPT condition is satisfied within a search time of 2 s. The algorithm then shifts to the adaptive P&O MPPT algorithm. It is observed that the particles initially oscillate with a certain magnitude which are subsequently damped to zero. The advantages of using the adaptive weight factor can be seen by the fact that there are almost negligible oscillations about the GP position once it is located as compared to the C-PSO algorithm.

The particle velocities involved when using the C-PSO and the proposed MPV-PSO are compared individually in Fig. 5c. From these graphs, it can be observed that for the MPV-PSO algorithm, the particle velocities never exceed a certain maximum limit. Thus, none of the peaks are skipped while searching for the GMPP. An added advantage is that the oscillations are of smaller amplitude; hence, a steady-state value close to zero is achieved much faster as compared to the C-PSO. At $t = 0.35$ s, the GMPPT condition is satisfied and the algorithm then shifts to the adaptive P&O MPPT. It is observed that the value of dP_{pv}/dV_{pv} is zero and thus PV voltage oscillation is zero.

Case II: The PSC-2 was chosen to ensure the middle peak among the three was the GP. Figs. 5d and e present the simulation results for this case. Compared to the nine cycles ($=27 \times T_{mpp}$) taken by the C-PSO algorithm to track the GMPP, the MPV-PSO algorithm takes only three cycles ($=9 \times T_{mpp}$). Here, one can notice the advantages of using the adaptive value for c_1 . In Fig. 5d, one particle initially gets trapped in one of the local minima, causing the convergence time to increase. However, in Fig. 5e, there is no evidence of any particle getting trapped at a local minimum and hence the quicker tracking performance. Table 3 provides all the simulation results conducted for static tracking in a tabular form.

Case III (dynamic GMPPT): In order to prove that the MPV-PSO algorithm has the capability of detecting changes in PSC and subsequently reinitialising itself to track the new GMPP, a simulation was conducted wherein the PSC was changed at some instant of time. A three-module PV string was considered for this simulation and the PSC was changed from PSC-2 to PSC-1. The simulation results are provided in Fig. 5f. The results prove that the algorithm is capable of tracking changes in the PSC and also make necessary compensations for the same.

5 Validation of proposed PSO-based GMPPT algorithm by hardware experiments

5.1 Hardware prototype description

A laboratory prototype, as shown in Fig. 6a, was developed to validate the hardware functionality of the proposed algorithm. Details of this prototype and parameters of the algorithm are given in Table 4. The P - V characteristics of the PV string are configured using a PV Simulator (Ametek make emulator and TerraSAS software). Hardware experiments have been carried out for different cases (Table 5) of static and varying PSC for series connected three and four module PV strings, using C-PSO and proposed MPV-PSO, and comparisons have been made.

5.2 Static global MPPT

Several hardware tests were conducted to prove that the MPV-PSO algorithm is successfully able to track the GP under PSC's and to highlight its better performance in comparison to the C-PSO algorithm. First, a three-module series string was subjected to the PSC-3. The P - V characteristics show three power peaks. Local peaks occur at (P_{L1} : 41.65 W, V_{L1} : 36.65 V), (P_{L2} : 23.12 W, V_{L2} : 17.77 V) and the GP is located at (P_g : 49.3 W, V_g : 56.33 V) as shown in Fig. 6b. For the purpose of searching the GP (P_g , V_g), the C-PSO as well as the proposed MPV-PSO GMPPT techniques are used. Fig. 6c shows the PV voltage (v_{pv}), PV current (i_{pv}) and power (P_{pv}) traces obtained by applying C-PSO. The PV voltage trace shows voltage oscillations with large step size during the initial searching cycles. This is undesirable because it causes the convergence time (T_{s_GMPPT}) to increase for tracking the GP. Next, the MPV-PSO algorithm is applied with adaptive values of w , c_1 and c_2 along with velocity limitation. Fig. 6d shows PV voltage, current and power traces obtained for this case. It can be observed that the step changes in voltage are small as compared to C-PSO and the convergence time is also reduced manifold. Also, the oscillations about the GP are non-existent for the case of MPV-PSO.

Another experiment was performed on the same PV string for the shading pattern of PSC-4. For this case, local peaks occur at (P_{L1} : 27.69 W, V_{L1} : 56.19 V), (P_{L2} : 21.93 W, V_{L2} : 17.65 V) and the GP is located at (P_g : 34.20 W, V_g : 36.37 V) as shown in Fig. 7a. Fig. 7b shows the GMPPT results using C-PSO algorithm, Fig. 7c depicts the same by applying MPV-PSO. For this PSC, it is found that by applying the MPV-PSO algorithm for GMPPT, the convergence time is greatly reduced. It also almost nullifies the oscillations about the GP, minimising power losses during steady-state operation. Fig. 7a shows the operating P - V characteristics of PV string under PSC-4 and highlights that the proposed MPV-PSO GMPPT tracks the GP with an efficiency of 99.95%.

In order to generalise the functionality of the MPV-PSO algorithm for any type of PV string, an experiment was performed for the PSC-5 with four PV modules in series. For this shading case, the local power peaks are located at (P_{L1} : 31.07 W, V_{L1} :

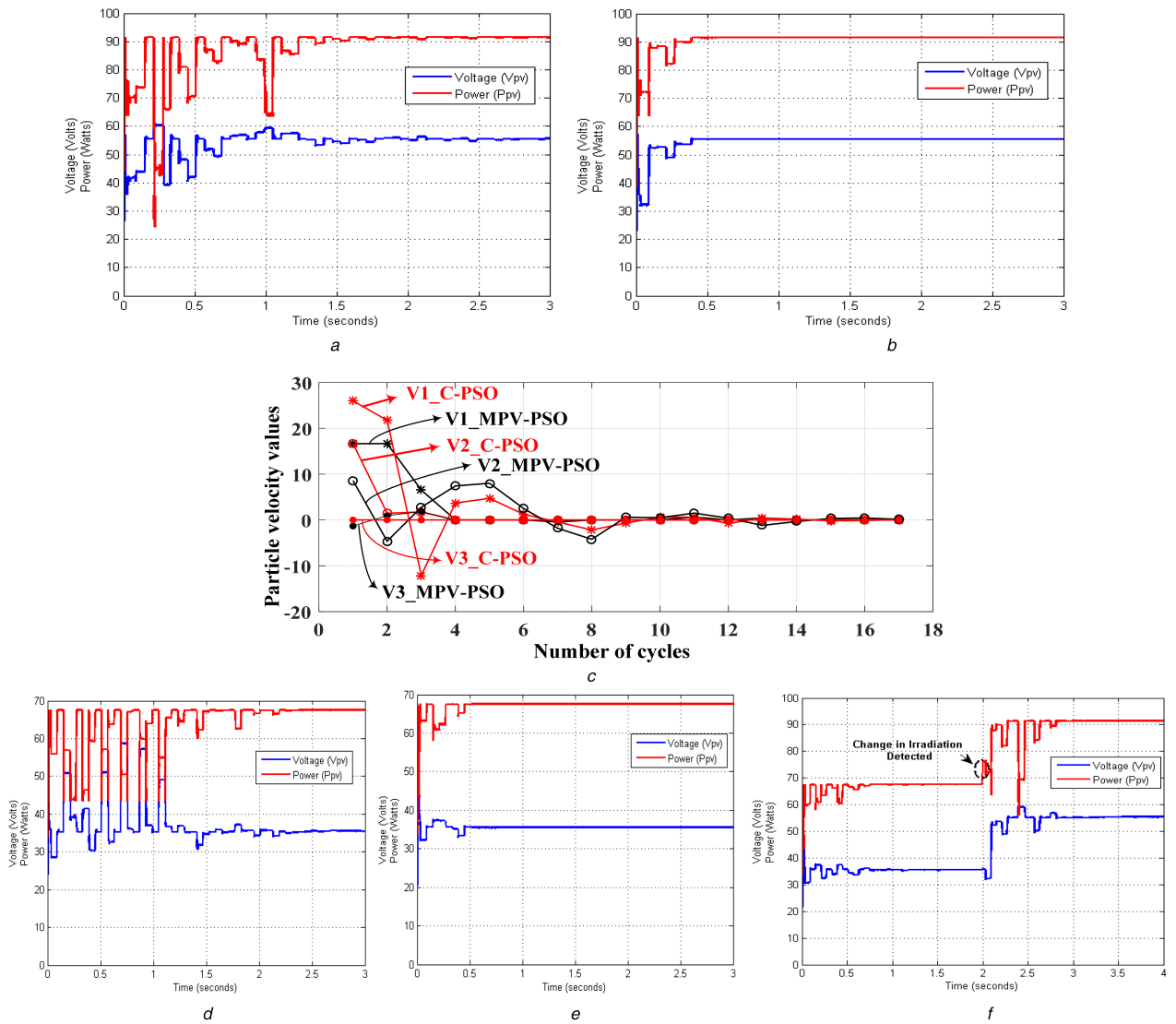


Fig. 5 Simulation results of PV array under PSC

(a) Power and voltage traces versus time for GMPPT by using conventional PSO algorithm for right peak PSC, (b) Power and voltage traces versus time for GMPPT by using proposed MPV-PSO algorithm for right peak PSC, (c) Graphical illustration and comparison of the individual particle velocities involved when using the conventional PSO and the proposed MPV-PSO algorithm for GMPPT for right peak PSC, (d) Using conventional PSO algorithm for middle peak PSC, (e) Using proposed MPV-PSO algorithm for middle peak PSC, (f) Using the proposed MPV-PSO algorithm for varying PSC's

Table 3 Summary of simulation results for static GMPP tracking

Number of modules	Shading configuration	Number of cycles taken by C-PSO to settle	Number of cycles taken by MPV-PSO to settle	Trapping in local minima for PSO	Trapping in local minima for MPV-PSO
3	PSC-1	10	3	No	No
3	PSC-2	9	3	Yes	No

42.39 V), (P_{L2} : 25.33 W, V_{L2} : 28.18 V) and (P_{L3} : 17.63 W, V_{L3} : 13.77 V) and the GP at (P_g : 34.12 W, V_g : 56.52 V) as shown in Fig. 7d. Fig. 7e shows the GMPPT using C-PSO, Fig. 7f presents the results for MPV-PSO. Similar improvements are present in the results for this PSC as were seen in the previous cases. It is also apparent from the hardware results shown that the C-PSO is unable to track the GMPP in this case, because there is no velocity limiting factor. On the other hand, the MPV-PSO successfully tracks the GP and the MPPT efficiency was measured to be 99.69%.

5.3 Dynamic global MPPT

The MPV-PSO is well suited for GMPPT under erratic variation of PSCs. The array was subjected to changing PSCs varying in the sequence PSC-6, PSC-7 and PSC-6 again as shown in Fig. 8, with the changes occurring after irregular intervals of time at t_1 , t_2 and

t_3 , respectively. At time instant t_1 , PV array is subjected to PSC-6. At the same time, the algorithm begins to track the GP and takes three cycles to do so. At t_2 , the irradiation levels incident on the PV array, change suddenly to PSC-7. This change is detected by the algorithm as there is a change in the PV array output power ($\Delta P_{pv} = 17.4$ W) which is more than P_{crit_s} , without there being any large change in the operating voltage. Immediately, the algorithm parameters are reinitialised and the search process is rerun. Finally, the irradiation levels incident on the array change back to PSC-6 at t_3 . As a result, the algorithm is reinitialised again for tracking the new GP, as defined previously. This experiment shows that the proposed MPV-PSO algorithm is capable of dynamic tracking, which means that it can track changes in the PSC and subsequently track the varying GP.

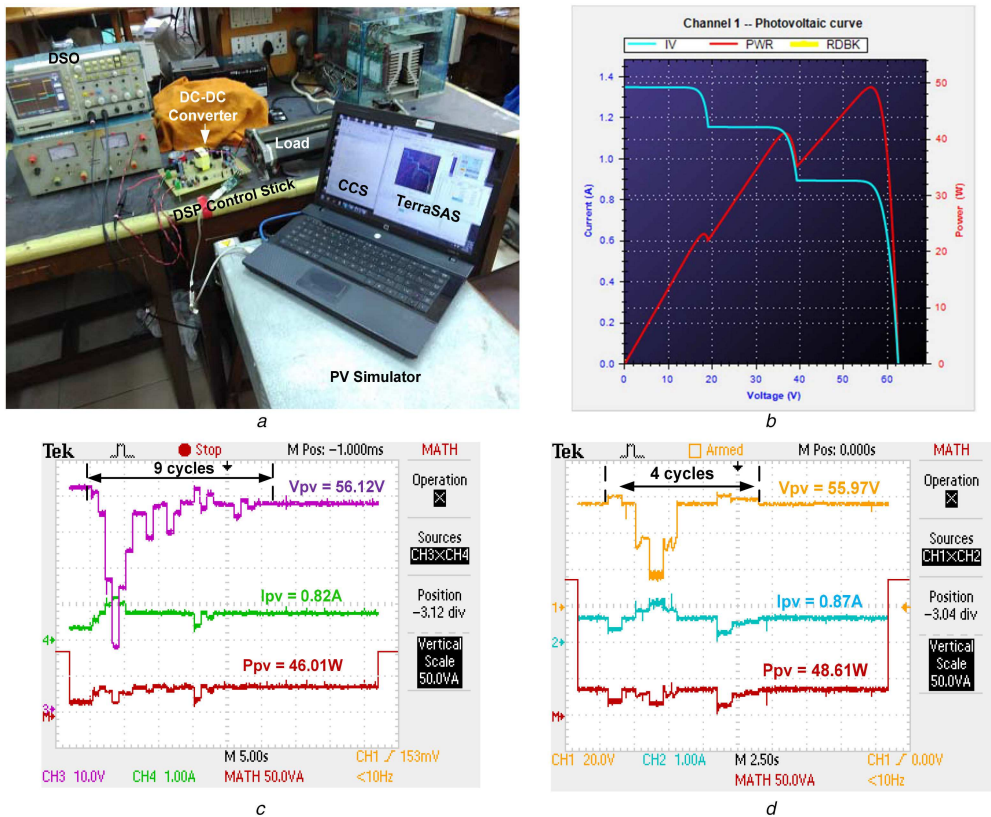


Fig. 6 Experimental results for GMPPT (shown by the voltage (v_{pv}), current (i_{pv}) and power (p_{pv}) traces) of PV string with three modules in series for right peak configuration

(a) Hardware setup used for tracking the GP of PV arrays using the MPV-PSO algorithm, (b) P-V characteristics for the PSC-3, (c) C-PSO algorithm, (d) MPV-PSO algorithm

Table 4 Hardware prototype details

Components	Symbols	Specifications
PV source	AMETEK PV simulator	PV module: $V_{OC} = 21\text{ V}$, $I_{SC} = 1.35\text{ A}$, $V_{MPP} = 18.1\text{ V}$, $I_{MPP} = 1.27\text{ A}$, $P_{MPP} = 22.987\text{ W}$
DSP control stick		TMS320F28069
power switch	S	IRFP460 (MOSFET)
power diode	D	MUR1560T
Inductor	L	3 mH
resistance (load)	R_{out}	200 Ω , 2.8 A
capacitors	C_{out}	100 μF , 200 V
	C_{PV}	100 μF , 200 V
C-PSO algorithm		$w = 0.4$, $c_1 = 1.0$, $c_2 = 1.5$
proposed MPV-PSO algorithm		w , c_1 and c_2 change adaptively depending on the particle position as per (6)

Table 5 Different shading patterns considered for experimental validations

GMPPT	No. of PV modules in a string	Shading pattern	PV#1, kW/m ²	PV#2, kW/m ²	PV#3, kW/m ²	PV#4, kW/m ²
static GMPPT	3	PSC-3	1	0.85	0.65	—
		PSC-4	0.954	0.695	0.352	—
	4	PSC-5	1	0.68	0.55	0.44
		PSC-6	0.95	0.8	0.6	—
dynamic GMPPT	3	PSC-7	0.954	0.695	0.352	—

6 Conclusions

In this paper, a modified particle velocity-based PSO algorithm has been proposed and verified for GMPP tracking of a PV array under PSC. The proposed PSO algorithm employs a modified update velocity equation for the particles in which the weight factor, the cognitive acceleration coefficient and the social acceleration coefficient change adaptively according to the particle position in the search space for achieving fast convergence, avoiding oscillations about the GP and successfully negotiating local minima. The algorithm also does away with the inherent

randomness by removing the random numbers from the velocity equation. In addition to this, the particle velocity is bounded by a certain upper limit, the value of which is based on the PV string's open circuit voltage. Extensive experimentation has been performed to validate the performance of the proposed scheme in contrast with the conventional PSO algorithm. These results show that the proposed MPV-PSO-based GMPPT technique performance better than conventional PSO-based scheme. The MPV-PSO can track the GP for any shading pattern with faster convergence and with smaller variation in the PV voltage and power during searching, ensuring higher tracking efficiency. The algorithm is

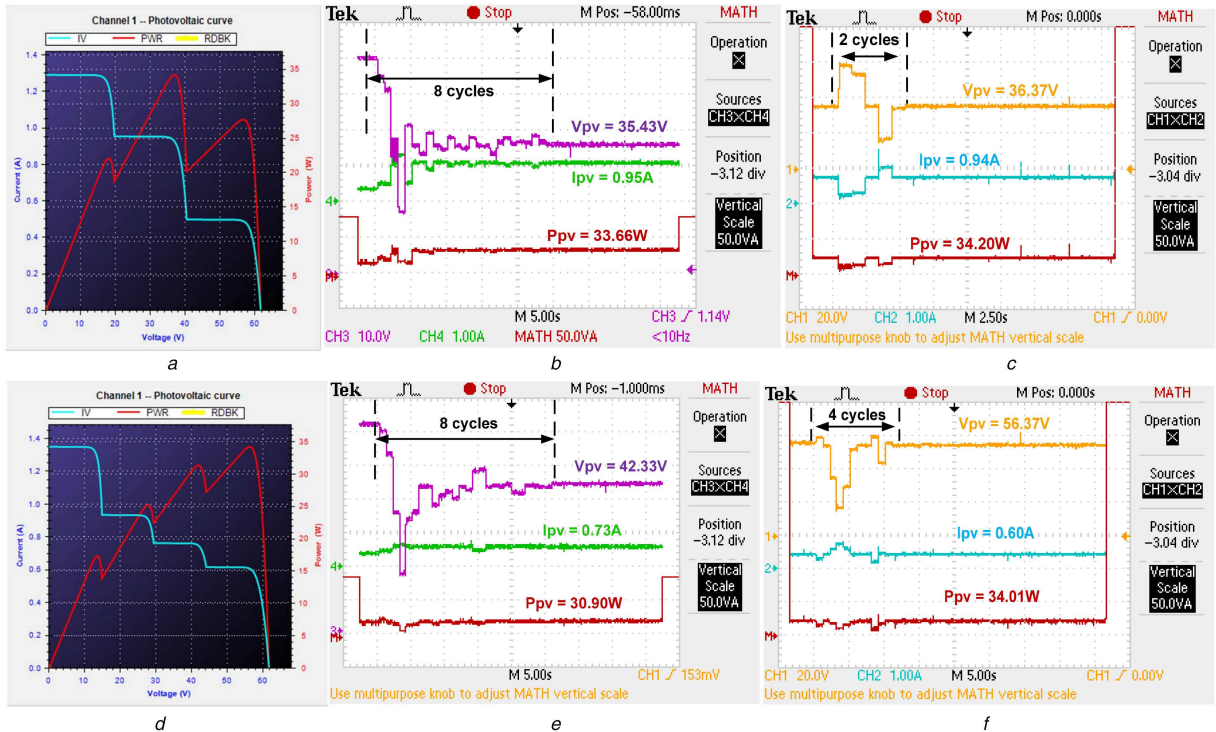


Fig. 7 Experimental results for GMPPPT (shown by the voltage (v_{pv}), current (i_{pv}) and power (p_{pv}) traces) of PV string under PSC

(a) $P-V$ characteristics for the three module PV string under PSC-4, (b) Conventional PSO algorithm for PSC-4, (c) MPV-PSO algorithm for PSC-4, (d) $P-V$ characteristics for the PSC-5, (e) Conventional PSO algorithm for PSC-5, (f) MPV-PSO algorithm for PSC-5

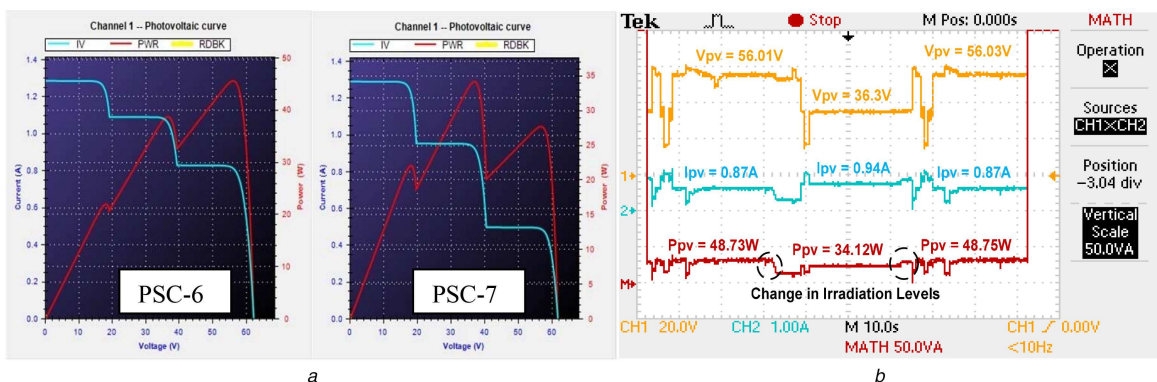


Fig. 8 Experimental results showing the GP tracking capability of the MPV-PSO algorithm under varying shading conditions for a three-module PV string
(a) From PSC-6 to PSC-7, (b) From PSC-6 to PSC-6 again

also capable of detecting changes in PSCs and tracking the varying GMPP. In addition to this, the GMPP efficiency of the MPV-PSO method is more than 99% for any shading condition.

7 References

- [1] Esram, T., Chapman, P.L.: 'Comparison of photovoltaic array maximum power point tracking techniques', *IEEE Trans. Energy Convers.*, 2007, **22**, (2), pp. 439–449
- [2] Houssamo, I., Locment, F., Sechilariu, M.: 'Maximum power tracking for photovoltaic power system: development and experimental comparison of two algorithms', *IET Renew. Energy*, 2010, **35**, pp. 2381–2387
- [3] Faraji, R., Rouholamini, A., Naji, H.R., et al.: 'FPGA-based real time incremental conductance maximum power point tracking controller for photovoltaic systems', *IET Power Electron.*, 2014, **7**, (5), pp. 1294–1304
- [4] Mohd Zainuri, M.A.A., Mohd Radzi, M.A., Soh, A.C., et al.: 'Development of adaptive perturb and observe-fuzzy control maximum power point tracking for photovoltaic boost dc-dc converter', *IET Renew. Power Gener.*, 2014, **8**, (2), pp. 183–194
- [5] Andrejasic, T., Jankovec, M., Topic, M.: 'Comparison of direct maximum power point tracking algorithms using EN 50530 dynamic test procedure', *IET Renew. Power Gener.*, 2011, **5**, (4), pp. 281–286
- [6] Jain, S., Agarwal, V.: 'Comparison of the performance of maximum power point tracking schemes applied to single-stage grid-connected photovoltaic systems', *IET Electr. Power Appl.*, 2007, **1**, (5), pp. 753–762
- [7] Tafticht, T., Agbossou, K., Doumbia, E.L., et al.: 'An improved maximum power point tracking method for photovoltaic systems', *IET Renew. Energy*, 2008, **33**, pp. 1508–1516
- [8] Patel, H., Agarwal, V.: 'Maximum power point tracking scheme for PV systems operating under partially shaded conditions', *IEEE Trans. Ind. Electron.*, 2008, **55**, (4), pp. 1689–1698
- [9] Syafaruddin Karatepe, E., Hiyama, T.: 'Artificial neural network-polar coordinated fuzzy controller based maximum power point tracking control under partially shaded conditions', *IET Renew. Power Gener.*, 2009, **3**, (2), pp. 239–253
- [10] Koutoulis, E., Blaabjerg, F.: 'A new technique for tracking the global maximum power point of PV arrays operating under partial-shading conditions', *IEEE J. Photovolt.*, 2012, **2**, (2), pp. 184–190
- [11] Nguyen, T.L., Low, K.S.: 'A global maximum power point tracking scheme employing DIRECT search algorithm for photovoltaic systems', *IEEE Trans. Ind. Electron.*, 2010, **57**, (10), pp. 3456–3467
- [12] Kobayashi, K., Takano, I., Sawada, Y.: 'A study on a two stage maximum power point tracking control of a photovoltaic system under partially shaded insolation conditions', Proc. IEEE Power Eng. Soc. General Meeting, July 2003, pp. 2612–2617
- [13] Boztepe, M., Guinjoan, F., Velasco-Quesada, G., et al.: 'Global MPPT scheme for photovoltaic string inverters based on restricted voltage window search algorithm', *IEEE Trans. Ind. Electron.*, 2014, **61**, (7), pp. 3302–3312
- [14] Ishaque, K., Salam, Z., Amjad, M., et al.: 'An improved particle swarm optimization (PSO)-based MPPT for PV with reduced steady-state oscillation', *IEEE Trans. Power Electron.*, 2012, **27**, (8), pp. 3627–3638
- [15] Jhang, J.H., Tian, I.S.: 'A maximum power tracking method based on perturb-and-observe combined with particle swarm optimization', *IEEE J. Photovolt.*, 2014, **4**, (2), pp. 626–633
- [16] Ishaque, K., Salam, Z.: 'A deterministic particle swarm optimization maximum power point tracker for photovoltaic system under partial shading condition', *IEEE Trans. Ind. Electron.*, 2012, **60**, (8), pp. 3195–3206

- [17] Liu, Y.H., Huang, S.C., Huang, J.W., *et al.*: ‘A particle swarm optimization-based maximum power point tracking algorithm for PV systems operating under partially shaded conditions’, *IEEE Trans. Energy Convers.*, 2012, **27**, (4), pp. 1027–1035
- [18] Clerc, M., Kennedy, J.: ‘The particle swarm – explosion, stability, and convergence in a multidimensional complex space’, *IEEE Trans. Evol. Comput.*, 2002, **6**, (1), pp. 58–73
- [19] Kollimala, S.K., Mishra, M.K.: ‘Variable perturbation size adaptive P&O MPPT algorithm for sudden changes in irradiance’, *IEEE Trans. Sustain. Energy*, 2014, **5**, (3), pp. 718–728
- [20] Villalva, M.G., de Siqueira, T.G., Ruppert, E.: ‘Voltage regulation of photovoltaic arrays: small-signal analysis and control design’, *IET Power Electron.*, 2010, **3**, (6), pp. 869–880